Novel Conducting Polymers for DNA Sensing

Hui Peng, Christian Soeller, and Jadranka Travas-Sejdic*

Polymer Electronics Research Centre, The University of Auckland, Private Bag 92019, Auckland, New Zealand

Received September 5, 2006; Revised Manuscript Received December 5, 2006

ABSTRACT: Novel functionalized pyrroles, 3-pyrrolylacrylic acid (PAA), 5-(3-pyrrolyl) 2,4-pentadienoic acid (PPDA), and 3-pyrrolylpentanoic acid (PPA) were synthesized and used to construct label-free gene sensors based on pyrrole copolymer films. Electrochemical impedance spectroscopy (EIS) was used to obtain electrical readout from these gene sensors. Comparison of the performance of PPDA-containing sensors to that containing 3-pyrrolylpentanoic acid (PPA), a similar functionalized pyrrole but with a saturated side chain, showed that functionalized polymers with unsaturated side chains have superior properties for use in biosensor applications. Sensors based on copolymers of both PAA and PPDA were evaluated across a wide range of oligonucleotide concentrations. The highest sensitivity was exhibited by a poly(Py-*co*-PPDA) sensor whose EIS spectra were well resolved, and the changes in charge-transfer resistance, taken as the index of sensor response, were largest among the materials studied. This sensor had a detection limit of 0.5 nM and a good selectivity.

Introduction

Gene analysis plays an ever-increasing role in a number of areas related to human health such as diagnosis of infectious diseases, genetic mutations, drug discovery, forensics, and food technology. To fulfill these challenges, a new generation of gene sensors that are fast, reliable, and cost-effective needs to be developed. Currently widely used gene array technologies rely on anchoring of specific probe DNA fragments or oligonucleotides (ODN) onto solid surfaces and detection of fluorescently or radioactively tagged analyte oligonucleotides that bind by Watson−Crick base pairing to the complementary probe sequence (hybridization). Such techniques have shortcomings arising from, for example, limited tagging efficiency, hazardous waste disposal, and complex multistep analysis. A number of novel approaches that seek faster, sensitive, and label-free gene detection have been suggested using new detection techniques based on optical,[1,2] acoustic,[3] and electrochemical[4−6] interactions.

Electrochemical gene sensors are regarded as particularly suitable for direct and fast biosensing since they can convert the biorecognition event (here DNA hybridization) into a direct electrical signal.[7−9] Electrochemical DNA sensing approaches include the intrinsic electroactivity of DNA,[10−13] electrochemistry of DNA-specific redox reporters,[14,15] electrochemistry of colloidal gold nanoparticles and nanocrystals,[16−18] and the electrochemistry of intrinsically conducting polymers.[8,19]

The intrinsically conducting polymers (ICPs) are a relatively new class of polymeric materials that possess a delocalized electronic structure which is sensitive to changes in the polymeric chain environment and other perturbations of chain conformation. Therefore, they may be used as active substrates that can sensitively report a biological recognition event, such as DNA hybridization. The changes in delocalized electronic structure or other ICP properties, caused by the recognition event, are manifested in altered optical and electrical properties of the ICPs and, when measured, can provide a signal for the presence of the target DNA sample.[20] For ICPs to be used as solid substrate for gene sensors oligonucleotides must be immobilized on or within the sensor film. Main immobilization methods include ODN entrapment,[21−23] covalent immobilization,[8,24−27] or affinity interactions.[28−30] Research into the covalent attachment of a biomolecule to amine- or carboxy-functionalized polymers was pioneered by Schuhmann.[31,32] Garnier et al. later proposed a process of functionalization of a conjugated polymer which involves the preparation of a precursor polymer film bearing a leaving group, such as an activated ester, at its 3-position, that can be substituted by an appropriate functional group.[26] Although several research groups investigated differently substituted pyrrole- or thiophene-based conducting polymers to prepare DNA sensors,[19,33,34] there is no study that investigates the effect of the "linker" group (functionalized side chain that links the polymer backbone and the bioprobe) on the resulting sensor properties.

Here we report the synthesis of monomers functionalized with unsaturated carbon side chains, 3-pyrrolylacrylic acid and 5-(3-pyrrolyl) 2,4-pentadienoic acid, and their conducting polymers. ODN probes were covalently attached to these polymers to construct gene sensors. We compare the response of one of the sensors having an unsaturated side chain with the response of a sensor based on a corresponding conducting polymer but with *saturated* side chains. Electrochemical impedance spectroscopy (EIS), which has been widely used for DNA detection,[6,35] was used to detect and quantify hybridization.

Experimental Section

Materials. Pyrrole (Py,), (triphenylphosphoranylidene) methyl acetate (TPPMA, 98%), $LiBH_4$ (95%), 1-ethyl-3-(3-(dimethylamino)propyl)carbodiimide (EDC), phosphate buffered saline pellets (PBS, pH 7.4), and propylene carbonate (anhydrous, 99.7%) were obtained from Aldrich. Pyrrole was distilled before use under vacuum. Invitrogen Life Technologies Co. synthesized the oligonucleotides (ODNs) including probe NH_2-GAT GAG TAT TGA TGC CGA-3′, complementary target 5′-TCG GCA TCA ATA CTC ATC-3′, one point mismatch 5′-TCG GCA ACA ATA CTC ATC-3′, two point mismatch 5′-TCG GCA AAA ATA CTC ATC-3′, and noncomplementary 5′-TAT GCT GGT GCG TCG CAC-3′. All aqueous solutions were prepared using Milli-Q water (18.2 MΩ·cm). Other chemicals used in this study were of reagent grade or better and purchased from local commercial sources. All reagents were used as supplied without further purification, unless otherwise stated.

* Corresponding author: e-mail j.travas-sejdic@auckland.ac.nz.

10.1021/ma062060g CCC: $37.00
Published on Web 01/19/2007

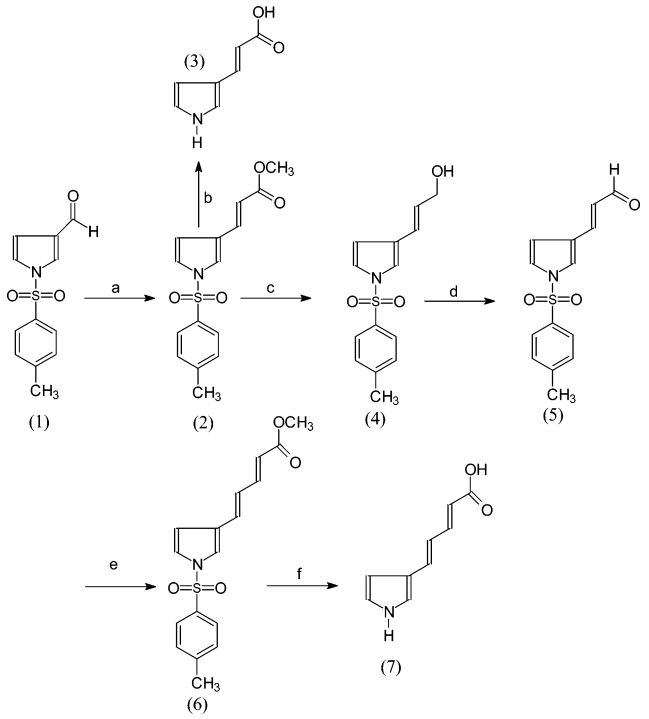

Figure 1. Synthesis of PAA and PPDA: (a) TPPMA, THF, 50 °C for 4 h; (b) MeOH/NaOH, refluxed for 5 h; (c) $LiBH_4$, THF, rt for 24 h; (d) MnO_2, chloroform, refluxed for 12 h; (e) TPPMA, THF, 50 °C for 4 h; (f) MeOH/NaOH, refluxed for 5 h.

Synthesis of 3-Pyrrolylacrylic Acid (PAA), 5-(3-Pyrrolyl)-2,4-pentadienoic Acid (PPDA), and 3-Pyrrolylpentanoic Acid (PPA). The synthesis of 1-(*p*-tolylsulfonyl)pyrrole-3-carboxaldehyde (**1**) was as previously described.[36] The subsequent synthesis steps are shown in Figure 1. A Wittig condensation between 1-(*p*-tolylsulfonyl)pyrrole-3-carboxaldehyde (**1**) and TPPMA proceeded to 3-(1-(*p*-tolylsulfonyl)pyrrol-3-yl)acrylic acid methyl ester (**2**), which was hydrolyzed to give PAA (**3**). ^{1}H NMR (DMSO-d_6): δ 5.95 (d,1H,), 6.40 (m, 1H), 6.80 (m, 1H), 7.18 (m, 1H), 7.46 (d, 1H,), 11.15 (s, 1H), 11.80 (s, 1H). IR (KBr): 3397 s, 2200−3500 br, 3436, 1691 m, 1663, 1603 s, 1498, 1410, 1338, 1272, 727 (see Supporting Information for ^{1}H NMR spectrum of 3-(3-pyrrolyl)acrylic acid).

3-(1-(*p*-Tolylsulfonyl)pyrrol-3-yl)-2-propenal (**5**) was obtained by reduction of 3-(1-(*p*-tolylsulfonyl)pyrrol-3-yl)-acrylic acid methyl ester (**2**) with $LiBH_4$ and oxidation of 3-(1-(*p*-tolylsulfonyl)pyrrol-3-yl)-2-propenol (**4**) with MnO_2. 3-(1-(*p*-Tolylsulfonyl)pyrrol-3-yl)-2-propenal (**5**) was subjected to Wittig condensation and hydrolysis to give PPDA (**7**). IR: 3424, 3500−2500, 1691, 1597, 1531, 1499, 1344, 1265, 1149, 1075, 989. ^{1}H NMR (DMSO-d_6, δ/ppm): 11.92 (s, 1H), 11.02 (s, 1H), 7.31 (m, 1H), 7.03 (m, 1H), 6.94 (d, 1H), 6.78 (m, 1H), 6.62 (m, 1H), 6.34 (m, 1H), 5.76 (d, 1H), 5.92 (d, 1H), 3.73 (s, 3H), 2.42 (s, 3H) (see Supporting Information for ^{1}H and ^{13}C NMR spectra of 5-(1*H*-pyrrol-3-yl)-2,4-pentadienoic acid).

The synthesis of 3-pyrrolylpentanoic acid (PPA) was performed according to the procedure by Cooper.[37]

Electrochemical Copolymerization. The electrochemical synthesis of poly(Py-*co*-PAA), poly(Py-*co*-PPDA), and poly(Py-*co*-PPA) films was carried out by using a CH Instrument electrochemical workstation (model 440, CH Instruments) at a fixed potential of 1.0 V (Ag/AgCl). A three-electrode cell with a volume of 3.0 mL, comprising a glassy carbon working electrode (BAS, 3.0 mm in diameter, 7.07 mm^2 geometrical area), an Ag/AgCl (3 M KCl) reference electrode, and Pt wire counter electrode, were used. Prior to electropolymerization, glassy carbon electrodes were polished with a 0.5 μm alumina slurry (Allied Tech Products, Inc.) and then washed with acetone, ethanol, and Milli-Q water. The polymerization solution contained 0.5 M Py, 6.25 mM PAA or PPDA, and 0.2 M $LiClO_4$ in 2 mL of acetonitrile or propylene carbonate. Film thickness was controlled by the total charge passed during polymerization.

Reflective FT-IR and UV−Vis Spectra Measurements. Reflective FT-IR spectra were measured using a Bio-RAD FTS-60 FT-IR spectrometer under a nitrogen atmosphere. For UV−vis spectral measurements, copolymer films were prepared in a solution containing 0.25 M Py, 0.025 M PAA or PPDA, and 0.2 M $LiClO_4$ in 2 mL of propylene carbonate on ITO quartz electrodes ($R_s = 15 \pm 5\ \Omega$, Delta Technologies, Limited). The UV−vis spectra of polymer films were recorded in situ in PBS solution at constant potential of 0.6 or −0.6 V using a UV-1700 spectrophotometer (Shimadzu).

ODN Probe Immobilization. The attachment of ODN probes onto the copolymer film was performed according to a previously described procedure.[38] To covalently attach the ODN probe, 40 μL of phosphate buffer (pH 5.2) containing 20 nmol of ODN probe and 400 nmol of EDC was applied to the surface of a copolymer-coated electrode and kept at 28 °C for 1 h. Finally, the modified electrode was thoroughly washed using PBS solution (pH 7.4) in order to remove any remaining unattached ODN probes.

Hybridization. Hybridization was carried out by incubating the sensor films in PBS solution (pH 7.4) containing ODN targets for 1 h at 42.0 °C, unless otherwise stated. After hybridization, the electrode was washed three times using PBS solution for 5 min to remove any nonhybridized ODNs.

Electrochemical Impedance Measurement. Electrochemical impedance spectra were recorded before and after hybridization using an EG&G potentiostat/galvanostat (model 280, Princeton Applied Research) coupled to an EG&G 1025 frequency response analyzer in PBS solution (pH 7.4) containing 5.0 mM $K_4Fe(CN)_6$/$K_3Fe(CN)_6$ (1:1 mol/mol) as a redox couple. Prior to measurements, all electrolyte solutions were purged for 5 min with nitrogen. A conventional three-electrode cell containing a modified glassy carbon electrode as working electrode, Pt slides as counter electrode, and Ag/AgCl (in 3 M KCl) as a reference electrode were used. The impedance experiments were run with a 10 mV sinusoidal excitation amplitude at an applied bias potential of 230 mV of the $[Fe(CN)_6]^{3-/4-}$ redox couple. The impedance data were measured and collected at harmonic frequencies from 1 Hz to 2 MHz at 12 steps per decade and analyzed using ZView software (version 2.80, Scribner Associates, Inc., North Carolina).

Results and Discussion

Copolymer Synthesis and Characterization. In previous ICP-based sensors, the "linker" between polymer backbone and DNA probe was a saturated alkyl chain.[8,19,33,34] Our primary motivation for this work was to investigate the difference in sensor responses arising from using conducting polymers that differ in saturation and length of the side chain.

Figure 1 shows the schematic of the synthesis of PAA and PPDA which contain unsaturated alkyl side chains. To our knowledge, synthesis of PPDA is reported for the first time, and a somewhat modified synthesis of PAA has been recently reported by us.[39]

The UV−vis spectra of pyrrole, PAA, and PPDA are shown in Figure 2. Compared with the UV spectrum of pyrrole, additional strong absorption peaks appeared in the spectra of PAA and PPDA at 300 and 335 nm, respectively. This is attributed to a $\pi-\pi^*$ transition of the double bond in the side chains of PAA and PPDA molecules. The unsaturated side chain UV absorption peak of PPDA is red-shifted compared to PAA, consistent with the expected increase of the effective conjugation length through $\pi-\pi^*$ delocalization.

Poly(Py-*co*-PAA) and poly(Py-*co*-PPDA) films produced by electropolymerization were investigated by means of reflective FTIR to confirm the presence of functionalized monomers in the copolymer through the presence of a band around 1710 cm^{-1}

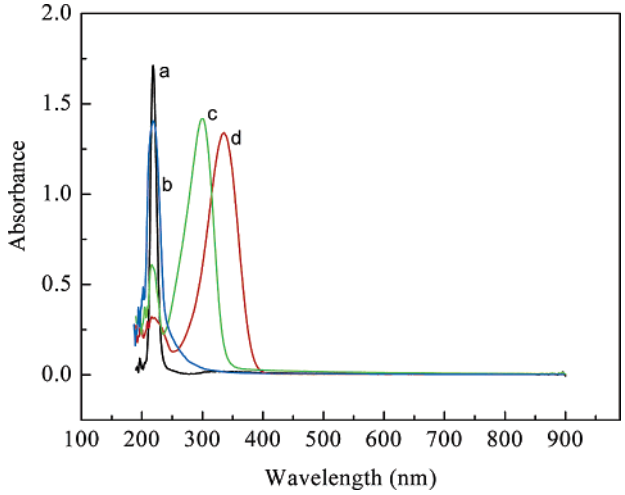

Figure 2. UV−vis spectra of monomers: (a) pyrrole, (b) 3-pyrrolylpentanoic acid (PPA), (c) 3-pyrrolylacrylic acid (PAA), (d) 5-(3-pyrrolyl)-2,4-pentadienoic acid (PPDA).

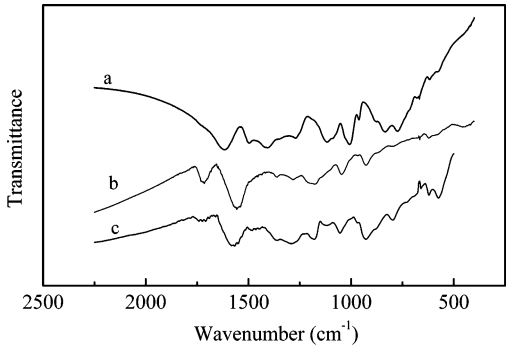

Figure 3. Reflective FT-IR spectra of polymer films: (a) PPy; (b) poly(Py-*co*-PAA); (c) poly(Py-*co*-PPDA).

due to the C═O stretching mode of the carboxylic group, as shown in Figure 3. To further confirm the presence of conjugated side chains, the UV−vis spectra of these copolymer films were measured (see Figure 3 of Supporting Information). Compared to PPy, poly(Py-*co*-PAA) and poly(Py-*co*-PPDA) have new absorption peaks at 292 and 307 nm, respectively, resulting from the presence of the conjugated side chains and consistent with the UV−vis spectra of PAA and PPDA monomers (see Figure 2). After reduction of films at −0.6 V, strong absorption peaks at 292 and 307 nm are still present, suggesting that the electrochemical reduction (or oxidation) only causes structural changes in the polymer backbone but does not disturb the conjugation between the side chains and the polymer backbone.

Performance of Sensors Based on Poly(Py-*co*-PPA) and Poly(Py-*co*-PPDA). In order to investigate the benefits of polypyrrole with conjugated side chains, we synthesized 3-pyrrolylpentanoic acid (PPA), which has a saturated side chain with the same number of carbons as PPDA. The copolymers of poly(Py-*co*-PPA) and poly(Py-*co*-PPDA) were electrochemically synthesized from a propylene carbonate solution of $LiClO_4$. The amino-functionalized ODN probes were covalently grafted on copolymer films by the well-known carbodiimide chemistry using EDC catalyst.[8] Changes in copolymer film characteristics following attachment of ODN probes and response to complementary ODN sequences were detected by means of electrochemical impedance spectroscopy (EIS) in PBS solution containing 5 mM $K_4Fe(CN)_6$/ $K_3Fe(CN)_6$ as a redox probe. The obtained electrochemical impedance spectra of the films are shown in Figure 4 (spectra a) in the form of Nyquist plots. All

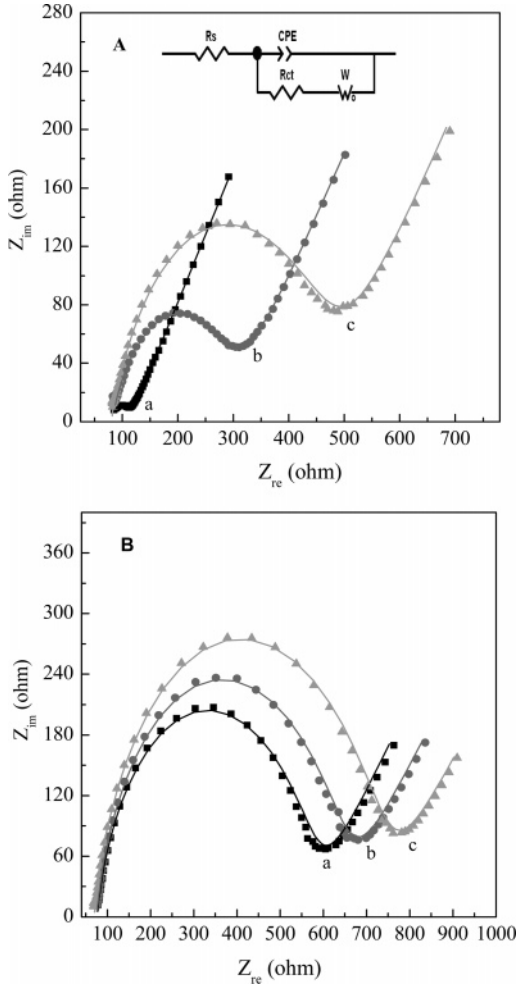

Figure 4. Nyquist plots ($-Z_{im}$ vs Z_{re}) for electrochemical impedance measurements based on electrodes coated with poly(Py-*co*-PPDA) (A) and poly(Py-*co*-PPA) (B) in PBS solution (pH 7.4) containing 5.0 mM $Fe(CN)_6^{3-}/Fe(CN)_6^{4-}$: (a) before immobilization of ODN probe; (b) after immobilization of ODN probe; (c) after incubation with 20.2 nM ODN target solution. Inset: equivalent circuit model. The experimental data are shown as symbols and the fitting data as solid lines.

spectra were fitted based on a modified Randles equivalent circuit that consists of a solution resistance (R_Ω) in series with a constant phase element (CPE) and Faradic impedance in parallel (as shown in Figure 5A, inset). The Faradic impedance consists of a charge-transfer resistance (R_{ct}) and a Warburg impedance (Z_ω). The inclusion of a CPE instead of a plain capacitance improved the goodness of fit. In physical terms a CPE (eq 1) reflects inhomogeneities of the surface reactions where the parameter n determines the extent of the deviation from the Randles and Ershler model:

$$CPE = A^{-1}(j\omega)^{-n} \tag{1}$$

When $n = 1$, the CPE reduces to a capacitance.[7] By using this model, the obtained charge-transfer resistance for poly(Py-*co*-PPA) and poly(Py-*co*-PPDA) films are 495 and 35 Ω, respectively. Significant difference in R_{ct} values obtained with those two films illustrates the improved electron-transfer capability of the poly(Py-*co*-PPDA) film as compared to a poly(Py-*co*-PPA) film.

Figure 4 also shows the electrochemical impedance spectra of poly(Py-*co*-PPDA) and poly(Py-*co*-PPA) films, after attachment of ODN probes (b) and after incubation in PBS solution containing 20.2 nM of complementary ODNs (c). After probe

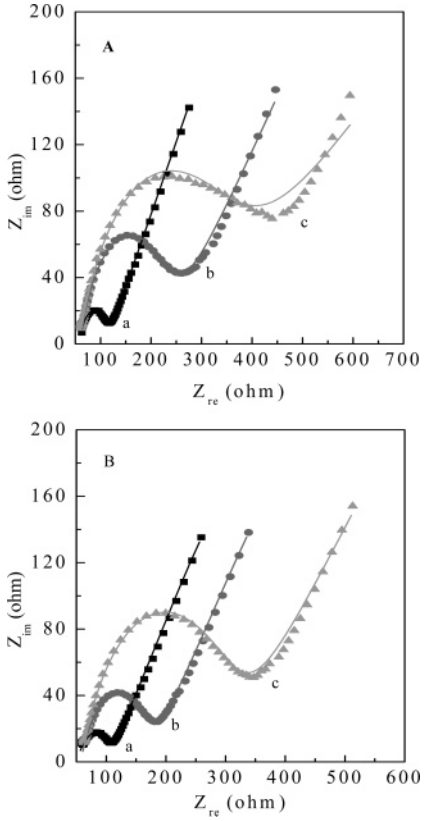

Figure 5. Nyquist plots ($-Z_{im}$ vs Z_{re}) for electrochemical impedance measurements based on electrodes coated with poly(Py-*co*-PAA) (A) and poly(Py-*co*-PPDA) (B) in PBS solution (pH 7.4) containing 5.0 mM $Fe(CN)_6^{3-}/Fe(CN)_6^{4-}$: (a) before immobilization of the ODN probes; (b) after immobilization of ODN probes; (c) after hybridization with 20.2 nM complementary ODNs. In all cases, the experimental data are shown as symbols and the fitting curves obtained with the equivalent circuit model as solid lines.

attachment, the values of R_{ct} increased in both materials due to the formation of a negatively charged ODN layer that electrostatically repels the negative redox probe, $[Fe(CN)_6]^{3-/4-}$, and inhibits interfacial electron transfer. The changes in the R_{ct} value for poly(Py-*co*-PPDA) and poly(Py-*co*-PPA) films were 184 and 67 Ω, respectively; i.e., the change in R_{ct} for the poly(Py-*co*-PPDA) film is more than twice that for the poly(Py-*co*-PPA) film. After hybridization with 20.2 nM complementary ODN, the ΔR_{ct} for poly(Py-*co*-PPDA) and poly(Py-*co*-PPA) films was 173 and 94 Ω, respectively. These results demonstrate that poly(Py-*co*-PPDA) films are much more susceptible to perturbations caused by probe immobilization and hybridization than an otherwise equivalent poly(Py-*co*-PPA) film. The primary difference in molecular structure between PPDA and PPA is the degree of side-chain conjugation. It is therefore reasonable to conclude from the above experiments that the presence of conjugation in the side chain improves the DNA sensor performance. A possible explanation is that the side chain of PPDA extends the polymer backbone conjugation toward the bioprobe through overlap of π electrons, which causes the whole electronic structure of the polymer to be more sensitive to perturbations caused by ODN hybridization. In addition, the negative charges on ODNs (and ODN duplexes) may cause strong deformation of the electron density of the side chains of PPDA, and this perturbation may be easily transferred to the polymer backbone via conjugation, thus providing a way of communication between the main polymer backbone and the probe ODN (or any other bioprobe) bound in the side chain.

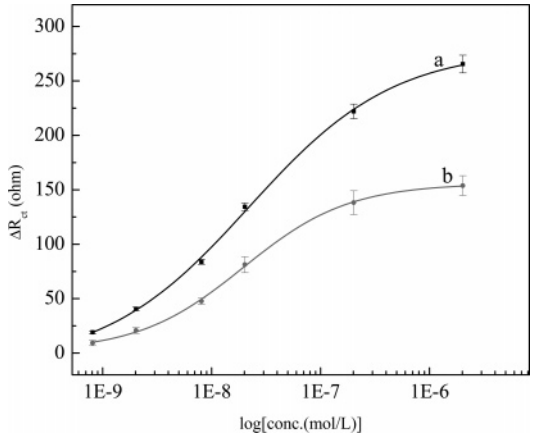

Figure 6. Calibration curves corresponding to the changes in charge-transfer resistance of electrodes modified with (a) poly(Py-*co*-PPDA) and (b) poly(Py-*co*-PAA) upon hybridization with different concentrations of the complementary ODN.

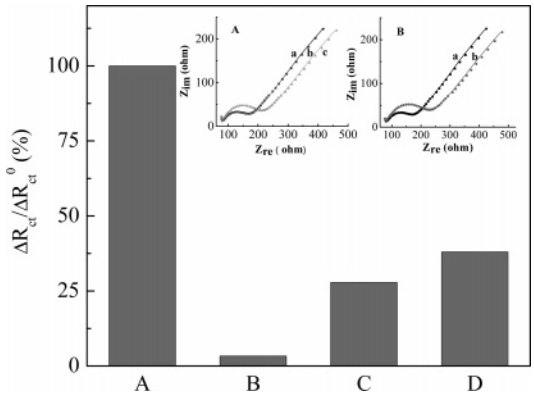

Figure 7. Normalized changes in the charge-transfer resistance of a sensor based on poly(Py-*co*-PPDA) film after hybridization with different ODN sequences (20.2 nM): (A) complementary ODN; (B) noncomplementary ODN; (C) two-point mismatched ODN; (D) one-point mismatched ODN. ΔR_{ct}^0 is the change in the charge-transfer resistance of the sensor hybridized with fully complementary ODN. Inset: (A) Electrochemical impedance spectra (a) after immobilization of ODN probe, (b) after incubation with 20.2 nM noncomplementary ODN, and (c) after incubation with 20.2 nM two-point mismatched ODN. (B) Electrochemical impedance spectra (a) after immobilization of ODN probe and (b) after incubation with 20.2 nM one-point mismatched ODN.

Comparison of Sensing Properties of Poly(Py-*co*-PAA) and Poly(Py-*co*-PPDA). The sensors based on poly(Py-*co*-PAA) and poly(Py-*co*-PPDA) films were prepared, and their sensing properties were investigated by EIS as described above. Parts A and B of Figure 5 present the electrochemical impedance spectra of poly(Py-*co*-PAA) and poly(Py-*co*-PPDA) films, respectively, directly after electropolymerization (a), after attachment of ODN probes (b), and after the sensors were incubated in PBS solution containing 20.2 nM of complementary ODNs (c). It can be seen from Figure 5 (curve a) that both copolymer films showed fast electron transfer. The charge-transfer resistance values, R_{ct}, are relatively small in both films, being 55 and 51 Ω for poly(Py-*co*-PAA) and poly(Py-*co*-PPDA), respectively. After ODN probe immobilization both films showed a significant increase in R_{ct}, presumably due to the formation of a negatively charged interface of ODNs that electrostatically repels the negative redox probe, $[Fe(CN)_6]^{3-/4-}$, and inhibits interfacial electron transfer. These findings are in general agreement with observations by Wallace et al.[40] and Wang et al.[41]

After hybridization the R_{ct} values increased further to 255.0 and 249.8 Ω for poly(Py-*co*-PAA) and poly(Py-*co*-PPDA), respectively. This can be explained by the formation of ODN duplexes that further distort the electronic properties of the polymer backbone and/or additional increase in the amount of electrostatic charges and thus the repulsion of the oppositely charged redox probe. When the change in charge-transfer resistance before and after hybridization, ΔR_{ct}, which was used as the sensor readout, is compared, poly(Py-*co*-PAA) has a response of 81.2 Ω and poly(Py-*co*-PPDA) of 134.4 Ω. The improved sensor response of poly(Py-*co*-PPDA) films illustrates that the longer side chain (5-carbon chain vs 3-carbon chain) has a positive effect on hybridization transduction. This result is in contrast to the study by Cooper et al., using polypyrroles with saturated side chains, on the heterogeneous electron-transfer rate constant of cytochrome *c* at the conducting polymer coated electrodes.[37] They found that the values of heterogeneous electron-transfer rate constant decreased significantly with the increase in the number of carbon atoms between the acid group and the pyrrole ring (i.e., side chain length). In this study, the electron-transfer capabilities of poly(Py-*co*-PAA) and poly(Py-*co*-PPDA) do not change as much with increasing side chain length most likely due to the conjugation between the side chain and polymer backbone, as demonstrated by the similar charge-transfer resistances of poly(Py-*co*-PAA) and poly(Py-*co*-PPDA) films (Figure 5, curve a). However, the increase in the length of the side chain, which acts as a "spacer", is expected to improve hybridization efficiency due to reduced steric constrains[42] which could be a reason for an increased poly(Py-*co*-PPDA) response.

Responses of both poly(Py-*co*-PAA) and poly(Py-*co*-PPDA) sensors to a range of concentrations of complementary ODNs were tested and are shown in Figure 6. The calibration curves have a sigmoidal shape with an approximately linear portion at concentrations from approximately 3×10^{-9} to 2×10^{-7} M. The ΔR_{ct} values for films based on poly(Py-*co*-PPDA) are larger in the whole range of concentrations investigated, especially at high concentrations of complementary ODNs confirming a positive effect of the longer side chain on the sensor response.

The sensitivities of sensors based on poly(Py-*co*-PAA) and poly(Py-*co*-PPDA) films were evaluated from the slopes of the linear part of the curves in Figure 6 and were 55 Ω/log[mol/L] and 86 Ω/log[mol/L] of complementary ODN, respectively. If the sensor response to a noncomplementary ODN target (20.2 nM) is considered as a noise, the resulting detection limits were 1 and 0.5 nM for poly(Py-*co*-PAA) and poly(Py-*co*-PPDA), respectively (S/N > 3).

Selectivity of the Sensor. The selectivity of the sensor based on poly(Py-*co*-PPDA) was investigated by measuring the response to several mismatched ODN targets. Figure 7 presents the normalized sensor response, $\Delta R_{ct}/\Delta R_{ct}^0$ (ΔR_{ct}^0 being the change in the charge-transfer resistance when hybridized with complementary ODN), for the various targets. The responses to one-mismatched, two-mismatched, and fully noncomplementary ODNs were 27, 38, and 3% of the signal for the fully complementary ODN target, respectively.

Conclusions

In this work, we synthesized two novel functionalized pyrrole monomers with unsaturated side chains, PAA and PPDA. Their copolymers with pyrrole were characterized by UV−vis and IR spectroscopy. Gene sensors based on poly(Py-*co*-PPA), poly(Py-*co*-PPDA), and poly(Py-*co*-PAA) films were prepared, and their performance was studied by EIS. The results imply that polypyrrole functionalized with unsaturated carbon side chains, onto which ODN probes are grafted, provides electrical-readout capable sensors with superior properties compared to a similar sensor that contains a saturated carbon side chain. We suggest that the most probable reason for such results is an extension of the polymer backbone conjugation toward the bioprobe through overlap of π electrons, which causes the whole electronic structure of the polymer to be more sensitive to perturbations caused by ODN hybridization. However, this should be investigated further to eliminate other possible effects (e.g., stiffness of the side chain). It was found that the longer side chain has a positive effect on the sensor response. The sensitivity and selectivity of the sensor based on poly(Py-*co*-PPDA) were investigated in detail, and the detection limit of 0.5 nM (S/N = 3) was determined along with a considerable sensor selectivity.

Acknowledgment. The authors thank the Marsden Fund (Royal Society New Zealand) and UniServices for financial support.

Supporting Information Available: Details of the synthesis of 3-pyrrolylacrylic acid and 5-(3-pyrrolyl)-2,4-pentadienoic acid and the UV−vis spectra of the copolymers. This material is available free of charge via the Internet at http://pubs.acs.org.

References and Notes

(1) Liu, J.; Tian, S.; Tiefenauer, L.; Nielsen, P. E.; Knoll, W. *Anal. Chem.* **2005**, *77*, 2756−2761.
(2) Peter, C.; Meusel, M.; Grawe, F.; Katerkamp, A.; Cammann, K.; Boerchers, T. *Fresenius' J. Anal. Chem.* **2001**, *371*, 120−127.
(3) Zhou, X. C.; Huang, L. Q.; Li, S. F. Y. *Biosens. Bioelectron.* **2001**, *16*, 85−95.
(4) Wang, J. *Electroanal. Methods Biol. Mater.* **2002**, 27−41.
(5) Alfonta, L.; Singh, A. K.; Willner, I. *Anal. Chem.* **2001**, *73*, 91−102.
(6) Katz, E.; Weizmann, Y.; Willner, I. *J. Am. Chem. Soc.* **2005**, *127*, 9191−9200.
(7) Katz, E.; Willner, I. *Electroanalysis* **2003**, *15*, 913−947.
(8) Peng, H.; Soeller, C.; Vigar, N.; Kilmartin Paul, A.; Cannell Mark, B.; Bowmaker Graham, A.; Cooney Ralph, P.; Travas-Sejdic, J. *Biosens. Bioelectron.* **2005**, *20*, 1821−1828.
(9) Wang, J. *Chem.—Eur. J.* **1999**, *5*, 1681−1685.
(10) Kerman, K.; Morita, Y.; Takamura, Y.; Tamiya, E. *Electrochem. Commun.* **2003**, *5*, 887−891.
(11) Karadeniz, H.; Gulmez, B.; Sahinci, F.; Erdem, A.; Kaya, G. I.; Unver, N.; Kivcak, B.; Ozsoz, M. *J. Pharm. Biomed.* **2003**, *33*, 295−302.
(12) Singhal, P.; Kuhr, W. G. *Anal. Chem.* **1997**, *69*, 4828−4832.
(13) Wang, J.; Rivas, G.; Fernandes, J. R.; Lopez Paz, J. L.; Jiang, M.; Waymire, R. *Anal. Chim. Acta* **1998**, *375*, 197−203.
(14) Millan, K.; Mikkelson, S. R. *Anal. Chem.* **1993**, *65*, 2317.
(15) Hashimoto, K.; Ito, K.; Ishimor, Y. *Anal. Chem.* **1994**, *286*, 219.
(16) Wang, J. *Anal. Chim. Acta* **2003**, *500*, 247−257.
(17) Cai, H.; Wang, Y.; He, P.; Fang, Y. *Anal. Chim. Acta* **2002**, *469*, 165−172.
(18) Wang, J.; Liu, G.; Polsky, R.; Merkoci, A. *Electrochem. Commun.* **2002**, *4*, 722−726.
(19) Garnier, F.; Korri-Youssoufi, H.; Srivastava, P.; Mandrand, B.; Delair, T. *Synth. Met.*. **1999**, *100*, 89−94.
(20) McQuade, D. T.; Pullen, A. E.; Swager, T. M. *Chem. Rev.* **2000**, *100*, 2537−2574.
(21) Wang, J.; Jiang, M.; Fortes, A.; Mukherjee, B. *Anal. Chim. Acta* **1999**, *402*, 7−12.
(22) Komarova, E.; Aldissi, M.; Bogomolova, A. *Biosens. Bioelectron.* **2005**, *21*, 182−189.
(23) Peng, H.; Soeller, C.; Cannell, M. B.; Bowmaker, G. A.; Cooney, R. P.; Travas-Sejdic, J. *Biosens. Bioelectron.* **2006**, *21*, 1727−1736.
(24) Livache, T.; Roget, A.; Dejean, E.; Barthet, C.; Bidan, G.; Teoule, R. *Nucleic Acids Res.* **1994**, *22*, 2915−2921.
(25) Lassalle, N.; Roget, A.; Livache, T.; Mailley, P.; Vieil, E. *Talanta* **2001**, *55*, 993−1004.
(26) Godillot, P.; Korri-Youssoufi, H.; Srivastava, P.; El Kassmi, A.; Garnier, F. *Synth. Met.* **1996**, *83*, 117−123.
(27) Cha, J.; Han, J. I.; Choi, Y.; Yoon, D. S.; Oh, K. W.; Lim, G. *Biosens. Bioelectron.* **2003**, *18*, 1241−1247.
(28) Rodrigez, L.-M. T.; Billon, M.; Roget, A.; Bidan, G. *J. Electroanal. Chem.* **2002**, *523*, 70−78.

(29) Dupont-Filliard, A.; Roget, A.; Livache, T.; Billon, M. *Anal. Chim. Acta* **2001**, *449*, 45−50.
(30) Bidan, G.; Billon, M.; Calvo-Munoz, M. L.; Dupont-Fillard, A. *Mol. Cryst. Liq. Cryst.* **2004**, *418*, 255−270.
(31) Schuhmann, W.; Lammert, R.; Uhe, B.; Schmidt, H. L. *Sens. Actuators, B* **1990**, *B1*, 537−541.
(32) Schuhmann, W.; Kranz, C.; Huber, J.; Wohlschlaeger, H. *Synth. Met.* **1993**, *61*, 31−35.
(33) Bidan, G.; Billon, M.; Galasso, K.; Livache, T.; Mathis, G.; Roget, A.; Torres-Rodriguez, L. M.; Vieil, E. *Appl. Biochem. Biotechnol.* **2000**, *89*, 183−193.
(34) Kang, S. K.; Kim, J.-H.; An, J.; Lee, E. K.; Cha, J.; Lim, G.; Park, Y. S.; Chung, D. J. *Polym. J.* (*Tokyo, Jpn.*) **2004**, *36*, 937−942.
(35) Katz, E.; Willner, I. *Springer Ser. Chem. Sens. Biosens.* **2004**, *2*, 67−116.
(36) Dong, X.; Ketcha, D. M. *Org. Prep. Proc. Int.* **1995**, *27*, 503−506.
(37) Ryder, K. S.; Morris, D. G.; Cooper, J. M. *Langmuir* **1996**, *12*, 5681−5688.
(38) Walsh, M. K.; Wang, X.; Weimer, B. C. *J. Biochem. Biophys. Methods* **2001**, *47*, 221−231.
(39) Hui Peng, C. S.; Vigar, N. A.; Caprio, V.; Travas-Sejdic, J. *Biosens. Bioelectron.*, in press (doi: 10.1016/j.bios.2006.07.010).
(40) Lu, W.; Nguyen, T. A.; Wallace, G. G. *Electroanalysis* **1998**, *10*, 1101−1107.
(41) Wang, J.; Jiang, M.; Mukherjee, B. *Anal. Chem.* **1999**, *71*, 4095−4099.
(42) Shchepinov, M. S.; Case-Green, S. C.; Southern, E. M. *Nucleic Acids Res.* **1997**, *25*, 1155−1161.

MA062060G